

# Mechanical, Microstructural and Tribo-Electrochemistry Characterization in Aqueous Media of Coatings Vanadium / Vanadium Nitride Used as Functional Coating for Implants

W. Aperador\*, J. Duque, E. Delgado

School of Engineering, Universidad Militar Nueva Granada, Bogotá-Colombia

\*E-mail: [g.ing.materiales@gmail.com](mailto:g.ing.materiales@gmail.com)

Received: 9 March 2016 / Accepted: 6 April 2016 / Published: 4 May 2016

---

The study presents tribo-electrochemistry properties of multilayers of Vanadium / vanadium nitride [V / VN] n (n = 1, 20, 50 and 100) deposited on surgical grade steel 316LVM through the Physical Vapor Deposition processes (PVD) using Magnetron Sputtering Technology. Nanoindentation tests were performed to determine the hardness of the coatings corrosion tests and assays tribocorrosion (synergy between corrosion and wear), which were carried out with equipment potentiostatic type adapted to a pin on disk tribometer also performed which was adapted to an electrochemical cell with three electrodes: A silver/silver chloride reference electrode (Ag/AgCl), a counter electrode of platinum and a working electrode immersed in a solution of ringers lactate at a temperature of 37 ° C. The evaluation of the tribo-corrosion testing was performed using the electrochemical technique potentiodynamic curve to calculate the value of polarization resistance Tafel polarization curves to determine the corrosion rate in the coatings. The characterization of microstructural and morphological subjected to fretting corrosion coatings it was performed using the technique of atomic force microscopy (AFM).

---

**Keywords:** Magnetron Sputtering, corrosion, Vanadium / vanadium nitride, tribo-corrosion, wear, atomic force microscopy, nanoindentation

## 1. INTRODUCTION

Vanadium is used to produce specialty steel alloys such as tool steels high speed, resistant to oxidation, for example: surgical instruments, tools, axes, bicycle frames, crankshafts, aircraft engines and gears are made of steel-reinforced vanadium [1]. Similarly, vanadium in its different forms such as vanadium pentoxide (V<sub>2</sub>O<sub>5</sub>), It used in the manufacture of ceramics and as a catalyst, vanadium dioxide is used to make glass coatings that block infrared radiation, Vanadium oxide is also used for the manufacture of jewelery, superconducting magnets of 175 000 gauss have vanadium between its components [2-3]. Nitride Vanadium (V), has a cubic crystal structure face-centered, the films grown

by magnetron sputtering VN have shown that this material has excellent mechanical and tribological properties, such as: High hardness, high melting point, good chemical resistance, good electrical conductivity, low coefficient of friction and other applications as protective coatings, diffusion barriers in microelectronics, resistant to corrosion and abrasion coatings, superconductors and decorative coatings, all these properties depend on the deposition parameters of the films [4-5]. Regarding applications vanadium nitride they highlight the solar control coatings, lubricants, barrier coatings, microelectronic devices and catalysts. Recently, They have been reported unique properties that make an electrochemical capacitor or VN suitable for applications supercapacitor charge storage devices indispensable in different fields such as: electrical systems for hybrid vehicles load leveling battery during startup, acceleration and braking, memory storage systems, generation potential required electronic components like cell, video recorders and digital telecommunications systems [6].

Regarding the tribological properties of vanadium-based alloys by nitrogen implantation nanoindentation tests reported. It has obtained an increased hardness in the near to 3 factor and ball tests on disk showed a decrease in the coefficient of friction in samples implanted in all the selected loads [7].

Some studies coatings have allowed the use of coatings as protection VN cutting tools, reason why, they studied the influence of the substrate temperature in film growth and morphology, likewise the behavior of the material was observed with respect to their electronic structure, density of electronic states and electrostatic potential, for this purpose different physical quantities such as dipole moments were calculated, spin density, to analyze the reactivity of the system bearing in mind the percentage of elements in the cell and the changes observed in its crystal structure [8-9]. By including aluminum and vanadium in the compound (TiAlV) N, these elements stabilize and increase their hardness GPa to 40, It is higher than that reported by the TiN 25.4 GPa, therefore for high temperature applications, the compound (TiAlV) N, promotes formation Magneli phases ( $V_xO_{3x-1}$ ), which offer a considerable decrease in the friction coefficient due to self-lubrication phenomena [10].

The films of VN, they are very sensitive to variations of the deposition parameters [11-12]. Therefore, when the bias voltage is increased polarization increased compressive stress and reduced crystallite size and grain size occurs. This is due to bombardment of Ar + ions of, which serves to flatten and compress the next film density of the substrate by high energy applied to the material surface, as a result of this effect the hardness and elastic modulus increase [13].

The aim of the research was to study the tribological properties of multilayers V / VN, Obtained surgical grade steels AISI 316LVM, by reactive magnetron sputtering using a single target, in order to observe the evolution of the hardness properties and morphology with the variation of the bilayers. For which the multilayers were grown V / VN by an automatic control of gas flow in the chamber magnetron sputtering.

## 2. EXPERIMENTAL METHODS

Surgical grade stainless steel is used, whose preparation is performed by means of abrasive paper silicon carbide different granulomere (80-1500), and the last step was the use of an abrasive

solution based on alumina to bring them to mirror shine. After the substrates were subjected to a cleaning process in an ultrasound system immersed in a sequence of ethanol and acetone for 15 minutes.

The coatings were obtained by physical vapor deposition technique (PVD) (DC magnetron sputtering) Using as a circular target 4 inch diameter Vanadium with a purity of 99.99%. Multilayer hard coatings Vanadium / vanadium nitride with 1, 20, 50 and 100 bilayers, a total coating thickness of 3  $\mu\text{m}$ .

The substrates were subjected for 15 minutes to a bias voltage of - 400 V (r.f.) with a power of 60 W (r.f) in a plasma of argon (Ar) to remove any oxide layer.

Similarly, an intermediate layer of V was deposited prior to deposition of VN, respectively, in order to increase the adhesion between the coatings and the substrate under a power r.f. 350 W. In an atmosphere composed of a mixture of argon and nitrogen the flow of the latter was set to 10 sccm. Before the growth of the films was chamber pressure of  $1 \times 10^{-2}$  mbar a voltage bias -30V a deposition rate of 180nm / h.

The surface analysis was conducted using Atomic Force Microscopy in contact mode (MFA); equipment used is a NaioAFM of NANOSURF, to measure the roughness of an area of 1986  $\mu\text{m}^2$ .

The hardness of the coatings was measured on a Hysitron system nanoindentation IT TriboIndenter 950. Berkovich diamond indenter type was used. The indenter operates as equilateral triangles and has a tip radius of 0.1  $\mu\text{m}$ . The conditions of application of the load was maximum load of 5 mN load, an approach speed: 1.8  $\mu\text{m} / \text{min}$ , a rate of loading and unloading of 0.01 mN / min, and five measurements were made on the coating. The method chosen to determine the hardness was developed by Oliver and Pharr (1992). Tribocorrosion characterization was performed of hard coatings multilayers wherein the corrosion behavior wear and corrosion-wear was evaluated, used as a reference standard stainless steel AISI 316 LVM. Assays tribocorrosion were carried out in a galvanostat potentiostat system marks Gamry PCI-4 for testing curves potentiodynamic polarization in a Pin-on-disk system (governed by the ASTM G99 standard, for testing wear) coupled to a three electrode electrochemical cell: a silver electrode silver (Ag / AgCl) chloride as reference electrode, a platinum counter electrode and the sample as working electrode; as Ringer's lactate corrosive medium solution was used.

**Table 1.** Test parameters for wear tests.

Parameter	Value
Pin or counterbody	Condyle bone
Diameter pin	6mm
Applied load	5N
Distance	100 m
Test speed	500rpm
Diameter of the trace	6mm
Temperature	(25 $^{\circ}\text{C}$ )

Through the technique potentiodynamic curves polarization resistance is determined, the polarization curves Tafel, corrosion potential and corrosion rate were obtained of 0.5 mV/s, an exposure area of 1 cm<sup>2</sup> and a range of potential from - 0.25 V to 1V.

For wear testing of each of the multilayer coatings test parameters of Table 1 they were taken into account.

After performing the tests corrosion and corrosion-wear structural characterization was performed, Morphological by technique of atomic force microscopy where morphology was observed measured in the worn in tribocorrosion of multilayer coatings.

### 3. RESULTS

#### 3.1 Atomic Force Microscopy of the Multilayers Surfaces

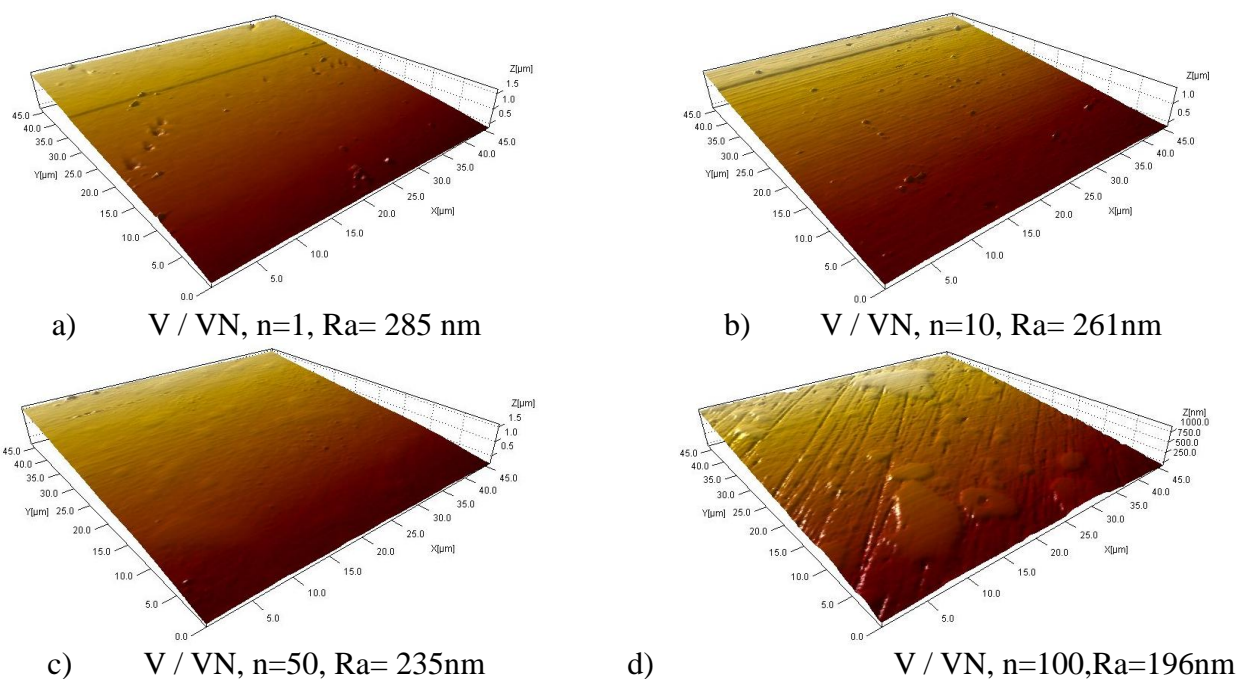


**Figure 1.** Atomic force micrographs corresponding to the samples obtained with different numbers bilayers the value of average roughness (Ra). a) n = 1, b) n = 20, c) n = 50 and n = 100.

In Figures 1 a to d, the surface morphology of multilayer coatings is observed, tests performed by atomic force microscopy (AFM), according to a more homogeneous topography measurements for coatings greater number of bilayers it is evident, this is for n = 100 bilayers, low roughness was obtained guarantees good coating performance against wear, therefore, any dislocation that is present on the surface of the film will fade as it moves toward the substrate, reducing the negative effect on this likewise the small grain size indicates that these types of coatings can be used as protective barriers of metal materials exposed to corrosive environments, since introducing the film borders of small grain, corrosive ions may not permeate solution coating easily to reach the substrate. Therefore the properties evident in the topography of the multilayer coatings (n) greater than 20 bilayers, will

give the substrate an increase in their lifetime and good mechanical and electrochemical performance [14-15].

In Figure 2, increasing the roughness of the layers 1 and  $n = 20$  is observed, this is due to the reaction of the surface with the wear-generating material, this is due to the structural nature, hardness and adhesion of multilayer coatings [16]. For systems with  $n = 50$  and  $n = 100$  show an increase in hardness as the bilayers number increases, which in turn causes grain growth with a result of increased hardness. Regarding this assay is to indicate that when having a surface with improved mechanical properties, because the number of bilayers showing the influence on the hardness of films, as seen this mechanical property decreases roughness, this behavior is maintained for systems with as many bilayers, point at which the hardness peaks [17-18]. AFM micrographs revealed that the low values of bilayers the surface of the films showed the dome structure, in those coatings deposited at high bilayers said structure presented. In films grown at  $n = 100$  was lost that structure [19]. These effects are explained in that as the number of bilayers, the kinetic energy of vanadium and argon ions is increased, producing and therefore harder denser structures [20]. Nevertheless, if the bilayers still increasing the structure collapses causing a decrease in hardness [21].

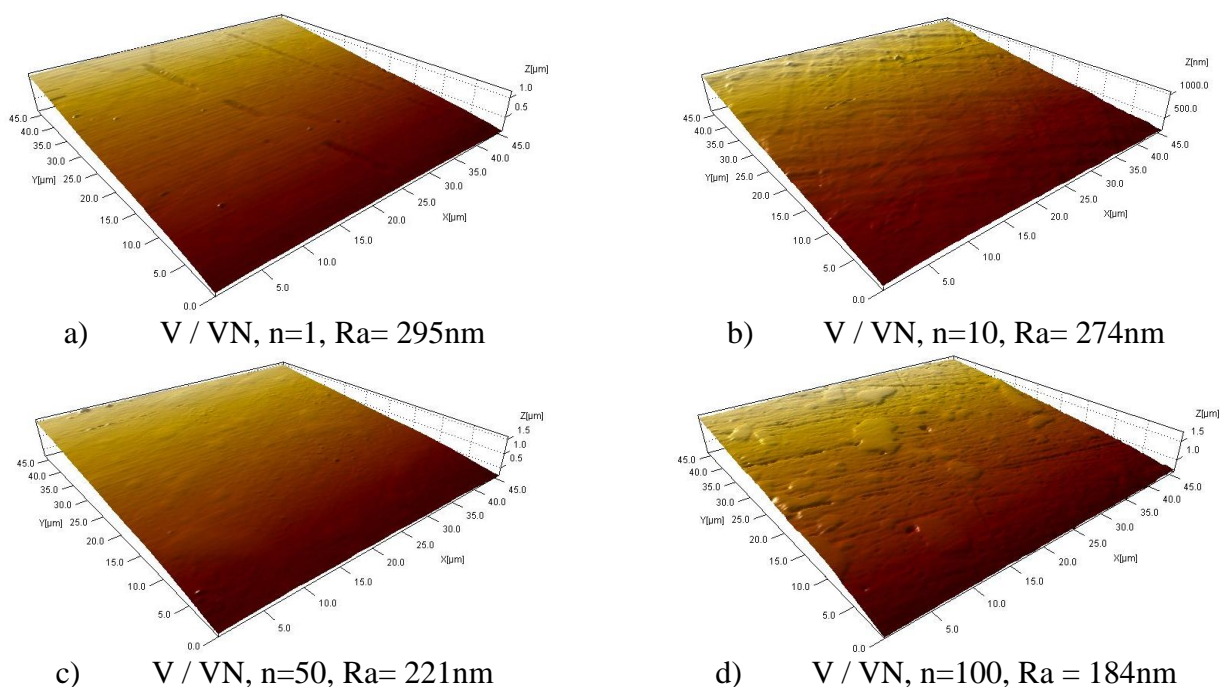


**Figure 2.** Atomic force micrograph mode noncontact thin films Vanadium / vanadium nitride post-test wear Pin on disk

In Figure 3, AFM micrographs observed the mixed wear corrosion test [21]. The main purpose of comparing the corrosion resistance of coatings of four types (Bilayer and multi-layer) for this purpose the tests were made using a tribometer adapted to system corrosion degradation [22]. You can see the behavior against Ringers solution electrolyte and the multilayers. The number accompanying the identification of coatings is the amount of deposited bilayers, by observing the images it is

concluded that the above coatings improved texture with respect to corrosion resistance as the number of bilayers is increased other side of the graphs of the multilayers were similar; although multilayers with  $n = 50$  to  $100$ , they showed less roughness due to corrosion degradation so it can be concluded that the best performance was achieved with  $100$  bilayers [23].

With the development of these materials it is seen as wear is mitigated by the effect of corrosion, therefore it may indicate that the characteristics such as wear resistance and corrosion; enhance protection of steel, due to deposit a multilayer Vanadium nitrides achieve adequate and significantly improve the corrosion resistance mechanical properties [23].

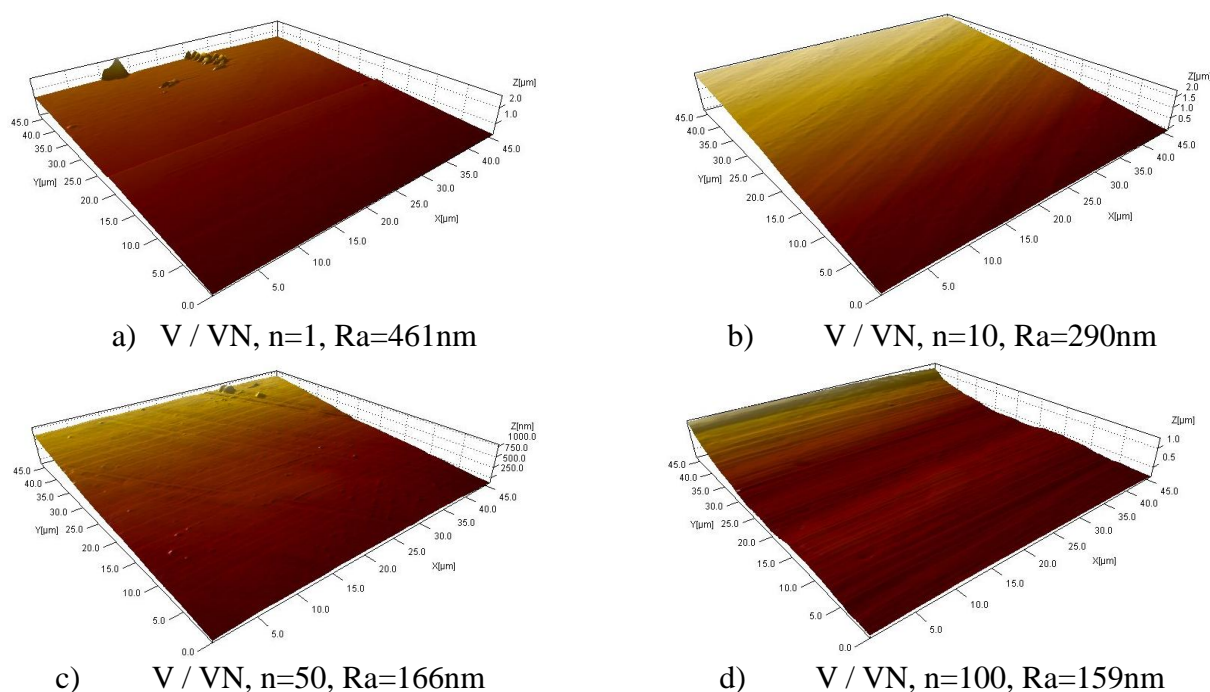


**Figure 3.** Determination by atomic force microscopy of the morphological change after exposure degradation, processes perform after test of the potentiodynamic curves in order to observe in more detail the wear suffered by the surfaces of each of the multilayers.

### 3.2 Hardness Measurements and Elastic Modulus by a Nanoindenter

In Figure 4, Hardness measurements of coatings made by the load curves is observed and download obtained in nanoindentation tests for multilayer coatings. Once obtained load curves and unloading of coatings under study hardness values and modulus were determined [24].

In curves it can be determined that the nitrogen content influences in the structure of vanadium nitride films therefore it is seen in the mechanical properties of the coatings, initially presents hardness increased multilayers going from  $1$  to  $20$  this behaviour is observed until  $100$  bilayer sat this point the hardness reaches its highest value, this is due to the presence of the intermediate layer of Vanadium [24].

The maximum hardness value it is because the film grains were randomly oriented [25]. The same graph shows the results of the adhesion test as in the case of said parameter hardness increases with the increase in multilayers interstitial nitrides have a definite structure and presents a chemical stability within these interstitial nitrides characteristics have a difference from electronegativity between nitrogen and vanadium and its atomic size allowing the nitrogen atoms are located more easily in the interstices of the crystal structure of metal such nitrides in metal bonds with some covalent and ionic components dominate. These characteristics give high hardness and generate the system is chemically inert.

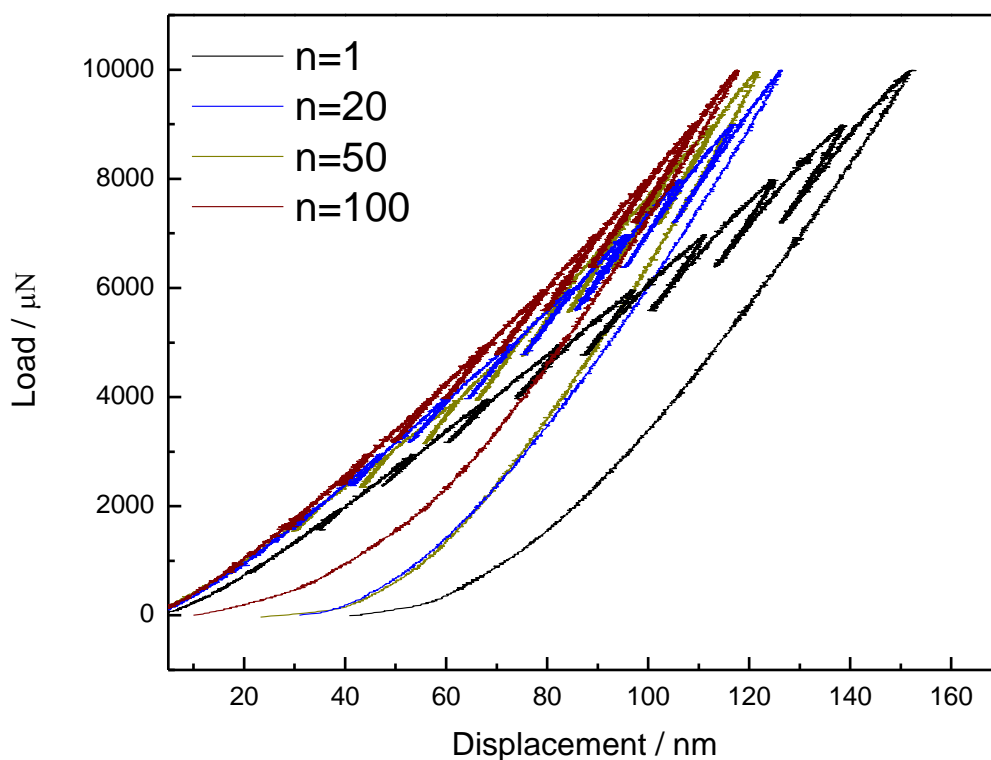


**Figure 4.** Typical Load Curve - Moving in a cycle of rigid tip nanoindentation in a semi-elastic space. To establish an analytical procedure; the relationship between the applied load  $P$  and displacement  $h$  elastic determines the elastic modulus of the multilayer coatings of  $V / VN$ .

From these values it can be deduced that the  $V / VN$  coatings they presented a value greater hardness and modulus of elasticity that increases as the number of bilayers obtaining the best estimates for multilayer coating with  $n = 100$  bilayers [26]. These results hardness and elastic modulus can be seen in more detail in Table 2.

The increase in the hardness values and modulus of elasticity is mainly due to the decrease in grain size and hence the low roughness which showed the coatings with increasing the number of bilayers since the surface of the deposited film becomes more homogeneous this can be demonstrated in the AFM micrographs of Figures 1, 2 and 3. Also, we can say that each bilayer gives rise to an

interface which acts as a barrier that prevents the propagation of dislocations through the grain boundaries [27].

A majority phase of vanadium nitride observed in multilayers VN phase associated with  $n = 100$ . It was evident that increasing multilayers V / VN the hardness of the steel AISI 316LVM, is improved there is a correlation between the decrease of grain size and hardness on the other hand multilayers roughness decreased with the number of bilayers.

**Table 2.** Hardness and elastic modulus of the multilayer coatings.

Material	Hardness $H$ (GPa)	Modulus of elasticity $E_r$ (GPa)
$n = 1$	29	282
$n = 20$	36	321
$n = 50$	38	342
$n = 100$	42	362

As the tribological properties of corrosive coatings Vanadium / vanadium nitride as multilayers have been studied because these materials are very hard; with hardness values found in this study in the range of 29 - 42 GPa Vickers (HV), Surface chemical interactions are of interest because they are in contact with Ringer's solution. As a result is obtained that the multilayers have a structure defined by the nature of its constituent atoms, this is important when considering the reactivity of the surface of said material as these indicate the mixed tribological behaviour both as protection against corrosion.

### 3.3 Tribocorrosion Testing Combined: Corrosion - Wear

The surface morphology of the multilayer coatings obtained by AFM, reflecting a homogeneous surface important feature for applications in wear resistance mechanical systems. They also showed that the multilayer system for V / VN the highest hardness values exceeding those found in single layer was obtained this is mainly because when the number of bilayers a large number of interfaces which have a resistance to movement of dislocations between each layer of VN is generated presenting a better resistance to corrosion [28]. Further, the multilayer system presented a 75% reduction in the friction coefficient compared to those of individual layers (Figure 5).

In Figure 5, the biomaterial useful as coatings due to their hardness is determined, chemical stability and wear resistance for this reason these multilayer coatings are considered hard because its hardness is greater or equal to 5 GPa and less than 40 GPa, coatings hardness greater than 40 GPa are called superhard, this for the case of 100 bilayers, because this aspect the best system is the one with the largest number of bilayers, since the modification of surgical grade steel surfaces 316LVM was achieved increasing the surface properties, the most prominent are: wear, friction and corrosion resistance. Tribocorrosion evaluation of properties of the coatings report low corrosion and wear values synergistically, generating protective properties, performance coatings and generate an adequate



contribution in improving the properties of the steel used as the substrate and therefore can predict the lifetime of different materials. These systems act as barriers against corrosion and wear in a system that simulates actual operating conditions.

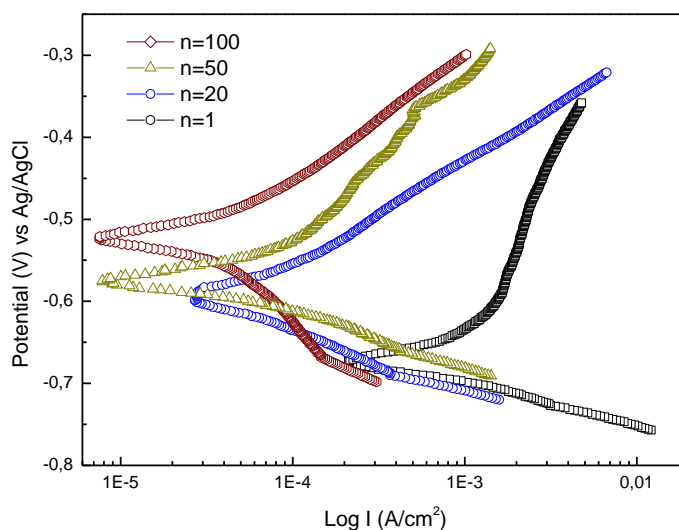


**Figure 5.** Potentiodynamic curves showing protection against corrosion and wear in thin films with variation the bilayers, indicating an appropriate behaviour for the purpose of use in applications such as biomaterials.

In Figure 5, the polarization curves where seen in the left branch of the four curves is observed wherein an active polarization is obtained (table 3), it is related to the activation energy needed to generate degradation, this energy is necessary for mechanical and electrochemical reaction, it is evident that a few layers there is a high corrosion rate, given to this high value the result of the energy barrier at the metal / electrolyte interface, however minimal increases as the number of bilayers is increased optimizing the value back to 50 layers. The value of the Tafel slope depends on the electrochemical reaction of the electrode surface and electrolyte, as there is a mixed system of electrochemical mechanical process and these values are high.

From the anodic-cathodic slopes calculated from Tafel polarization curves, we can calculate the corrosion current density  $i_{corr}$  by Stern-Geary equation (Equation 1).

$$i_{corr} = \frac{\beta_a \cdot \beta_c}{2.303R_p (\beta_a + \beta_c)} \tag{1}$$

where  $\beta_a$  and  $\beta_c$  are the anode and cathode Tafel slopes, respectively, and  $R_p$  is the polarization resistance. In turn, the  $i_{corr}$  is related to the corrosion rate through Faraday's law by expression:

$$V_{corr} = \frac{i_{Corr}KE_w}{d} \tag{2}$$

where  $K$  is a constant that defines the units of the corrosion rate,  $E_w$  is the equivalent weight of the working electrode in grams, and  $d$  is the density of the working electrode ( $\text{g}/\text{cm}^3$ ).

As it is known, corrosion behavior is not only due to the intrinsic properties of the coating, but also a result of small structural defects, such as pores and micro-cracks, formed during deposition.

**Table 3.** Polarization curves corresponding to the multilayers subject to wear; by pin on disk and additionally measure corrosion.

	$E_{\text{corr}} / \text{V}$	$I_{\text{corr}} / \mu\text{A cm}^2$	$V_{\text{corr}} / \mu\text{m y}$
n=1	-0.67	1290	1030.09
n=20	-0.59	111	88.63
n=50	-0.57	56.7	45.27
n=100	-0.52	30.9	24.67

### 3.4 Potentiodynamic polarization curves

In Figure 6, coatings were evaluated by potentiodynamic polarization the corrosion resistance of the multilayers when subjected to the action of the electrolyte ringer’s lactate.

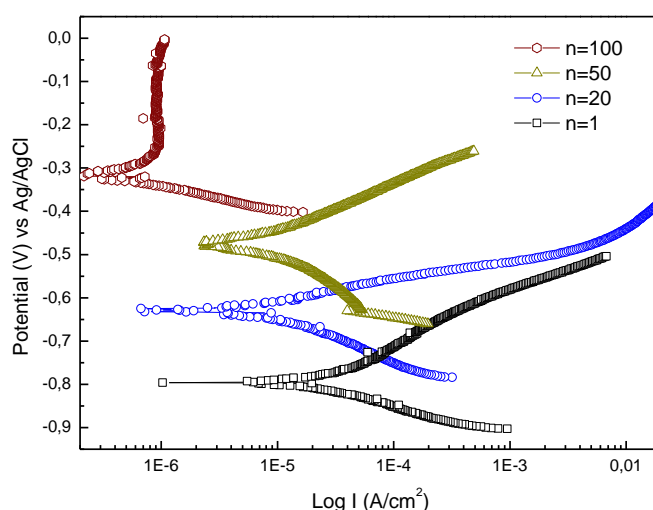


**Figure 6.** Polarization curves are observed where the polarization, these curves allow us to find the values of the anodic and cathodic currents outstanding in each case, which they are necessary for calculating an accurate value of the corrosion rate for each of the multilayers comparing this behaviour with the mixed mechanism of corrosion wear a decrease in the parameters is obtained.

It can be seen from the graph previous coatings exhibit improved behaviour in relation to the mixed system and tribological wear corrosion, in Tafel polarization curves the corrosion current for the multilayer coatings were determined with 1 bilayer recorded the highest value of current density ( $58.5 \mu\text{A}/\text{cm}^2$ ), followed by the layer of  $n = 20$  ( $19.2 \mu\text{A}/\text{cm}^2$ ) and  $n = 50$  which was  $9.26 \mu\text{A}/\text{cm}^2$ , while for layer  $n = 100$ ; was  $0.36 \mu\text{A}/\text{cm}^2$ , these values indicate the positive effect of depositing multilayers instead of individual layers [29]. Analysis of corrosion potential in turn indicates that nobler voltages are generated as the number of bilayers is increased meanwhile the multilayer of  $n = 100$ , He exhibited the best performance of the four coatings. However, knowing that the results of potentiodynamic polarization testing of the multilayer. Varying the  $i_{\text{corr}}$  and  $E_{\text{corr}}$  and the increased number of layers results when the number of layers increases from 20 to 100, the corrosion current decreases by two orders of magnitude, these values confirm the positive effect of the increase the number of layers.

The results show that the potentiodynamic tests without subjecting them to mechanical wear this is due to a dense and compact structure. This is because the individual layers of V and VN showed larger grain size in the multilayers to low bilayers which in turn it is attributed to processes re nucleation own deposition successive layers [30]. Another aspect that was found is about the behaviour of the films and the porosity, through observations by atomic force microscopy where micropores are present whose size was smaller in the multilayers with 50 and 100 bilayers, than in fewer bilayers. When comparing the results of static corrosion and fretting corrosion system with respect to the corrosion potential and passive current density, it is obtained that coatings provide better protection for the action of the electrolyte without the presence of mechanical wear. Thus the corrosion resistance relative to the Tribo-electrochemical system is improved, since in all trials they showed a nobler corrosion potential [29].

In Figure 6, better wear behaviour phenomenon is observed since only it intervenes corrosion the film presents a single bilayer appropriate behaviour and compared, is observed to 20 bilayers with a small potential variation due to changes in concentration in the immediate interface multilayers, this variation generates a protection reflected in the decrease in current and corrosion rate as compared with  $n = 1$  (table 4). The curves indicate there is an anodic dissolution so that the protective effect of the coating works properly not to present pitting corrosion.

**Table 4.** Measure corrosion rate by extrapolating the Tafel slopes for multilayers subjected to simulated fluid.

	$E_{\text{corr}} / \text{V}$	$i_{\text{corr}} / \mu\text{A cm}^2$	$V_{\text{corr}} / \mu\text{m}$
n=1	-0.79	70.1	55.97
n=20	-0.62	26	20.76
n=50	-0.47	1.8	1.43
n=100	-0.31	0.751	0.59

#### 4. CONCLUSION

The best wear resistance in steels were found to multilayers greater number of bilayers, similarly, the coefficient of friction on steel for multilayers decreased with the number of bilayers. This is because to the type of coating it is thin and it is consisting of very thin layers with a thickness of about 3 microns in the form of high quality multilayer structure both in composition and in the V / VN structure: By this study it was determined that this type of coating is functional surfaces are subjected to sliding and corrosion which would lead to an increase in the useful life of the coated material additionally if the system is not subjected to cyclic loads coatings increase resistance to corrosion due to their appropriate density.

#### ACKNOWLEDGEMENTS

Thanks the financial support from the Universidad Militar Nueva Granada, contract number ING-1903-2015.

#### References

1. J. Huotari, R. Bjorklund, J. Lappalainen, A. Lloyd Spetz, *Sens. Actuators, B*, 217 (2015) 22
2. M. Meenakshi, R. Sivakumar, P. Perumal, C. Sanjeeviraja, *Mater. Today: Proc*, 3 (2016) S30
3. D. Louloudakis, D. Vernardou, E. Spanakis, N. Katsarakis, E. Koudoumas, *Surf. Coat. Technol.*, 230 (2013) 186
4. J. Huotari, J. Lappalainen, J. Puustinen, A. Lloyd Spetz, *Sens. Actuators, B*, 187 (2013) 386
5. X.H. Zheng, D.G. Walmsley, *Physica C*, 515 (2015) 41
6. F.M. Bautista, J.M. Campelo, D. Luna, J. Luque, J.M. Marinas, *Catal. Today*, 128 (2007) 183
7. I. Mayrhuber, C.R. Dennison, V. Kalra, E.C. Kumbur, *J. Power Sources*, 260 (2014) 251
8. M.R. Tavakoli, D.B. Dreisinger, *Hydrometallurgy*, 141 (2014) 17
9. P.C. Rout, K. Sarangi, *Sep. Purif. Technol.*, 122 (2014) 270
10. R. Irmawati, M. Asri Razali, Y.H. Taufiq-Yap, Z. Zainal, *Catal. Today*, 93–95 (2004) 631
11. A. Held, J. Kowalska-Kuś, K. Nowińska, *Catal. Commun.*, 17 (2012) 108
12. A.S. Hassanien, Alaa A. Akl, *J. Alloys Compd.*, 648 (2015) 280
13. B. Krause, M. Kaufholz, S. Kotapati, R. Schneider, E. Müller, D. Gerthsen, P. Wochner, T. Baumbach, *Surf. Coat. Technol*, 277 (2015) 52
14. A.S. Hassanien, Alaa A. Akl, *Superlattices Microstruct.*, 89 (2016) 153
15. A. Abdel-Aal, The optical parameters and photoconductivity of  $Cd_xIn_{1-x}Se_{9-x}$  chalcogenide thin films, *Physica B*, 392 (2007) 180
16. K.M.A. Saron, M.R. Hashim, M.A. Farrukh, *Superlattices Microstruct*, 64 (2013) 88
17. H. Meidia, A.G. Cullis, C. Schönjahn, W.D. Münz, J.M. Rodenburg, *Surf. Coat. Technol.*, 151(2002) 209
18. J.C. Madaleno, G. Cabral, E. Titus, L. Pereira, J. Grácio, N. Ali, *Thin Solid Films*, 515 (2006) 106
19. M.A. Sumesh, Shivaprasada Karanth, Sharadadevi Prakash, A.S. Laxmiprasad, C.L. Nagendra, *Sens. Actuators, A*, 192 (2013) 81
20. A. Esmaili, *Procedia Eng.*, 42 (2012) 1634
21. M. Cloutier, C. Harnagea, P. Hale, O. Seddiki, F. Rosei, D. Mantovani, *Diamond Relat. Mater.*, 48 (2014) 65
22. M. Cloutier, D. Mantovani, F. Rosei, *Trends Biotechnol.*, 33 (2015) 637

23. B.J. McEntire, B.S. Bal, M.N. Rahaman, J. Chevalier, G. Pezzotti, *J. Eur. Ceram. Soc.*, 35, (2015) 4327
24. M. Mumjitha, V. Raj, *J. Mech. Behav. Biomed. Mater.*, 46 (2015) 205
25. G. Marchiori, N. Lopomo, M. Boi, M. Berni, M. Bianchi, A. Gambardella, A. Visani, A. Russo, M. Marcacci, *Mater. Sci. Eng., C*, 58 (2016) 381
26. A.P. Serro, C. Completo, R. Colaço, F. dos Santos, C. Lobato da Silva, J.M.S. Cabral, H. Araújo, E. Pires, B. Saramago, *Surf. Coat. Technol.*, 203 (2009) 3701
27. S.A. Naghibi, K. Raeissi, M.H. Fathi, *Mater. Chem. Phys.*, 148 (2014) 614
28. F. Toptan, A. Rego, A.C. Alves, A. Guedes, *J. Mech. Behav. Biomed. Mater.*, 61 (2016) 152
29. J. Ryan Stanfield, Stacy Bamberg, *J. Mech. Behav. Biomed. Mater.*, 35 (2014) 9
30. M.F. Montemor, R. Pinto, M.G.S. Ferreira, *Electrochim. Acta*, 54 (2009) 5179

© 2016 The Authors. Published by ESG ([www.electrochemsci.org](http://www.electrochemsci.org)). This article is an open access article distributed under the terms and conditions of the Creative Commons Attribution license (<http://creativecommons.org/licenses/by/4.0/>).